HAFO: Humanoid Force-Adaptive Control for Intense External Force Interaction Environments

Chenhui Dong^{a,b}, Haozhe Xu^{c,b}, Wenhao Feng^{c,b}, Zhipeng Wang^{a,b,c,d}, Yanmin Zhou^{a,b,c,d}, Yifei Zhao^{a,b}, Bin He^{a,b,c,d}

^aFrontiers Science Center for Intelligent Autonomous Systems, Tongji
University, Shanghai, 201109, China

^bNational Key Laboratory of Autonomous Intelligent Unmanned
Systems, Shanghai, 201109, China

^cDepartment of Control Science and Engineering, College of Electronics and Information
Engineering, Tongji University, Shanghai, 201804, China

^dShanghai AI Laboratory, Shanghai, 200030, China

Abstract

Reinforcement learning (RL) controllers have made impressive progress in humanoid locomotion and light load manipulation. However, achieving robust and precise motion with strong force interaction remains a significant challenge. Based on the above limitations, this paper proposes HAFO, a dual-agent reinforcement learning control framework that simultaneously optimizes both a robust locomotion strategy and a precise upper-body manipulation strategy through coupled training under external force interaction environments. Simultaneously, we explicitly model the external pulling disturbances through a spring-damper system and achieve fine-grained force control by manipulating the virtual spring. During this process, the reinforcement-learning policy spontaneously generates disturbance-rejection response by exploiting environmental feedback. Moreover, HAFO employs an asymmetric Actor-Critic framework in which the Critic-network access to privileged spring-damping forces guides the actor-network to learn a generalizable, robust policy for resisting external disturbances. The experimental results demonstrate that HAFO achieves stable control of humanoid robot under various strong force interactions, showing remarkable performance in load tasks while ensuring stable robot operation under rope tension disturbances. Project website: http://hafo-robot.github.io.

Keywords: Force-Adaptive Control, Whole body control, Reinforcement

1. Introduction

In recent years, RL-based control solutions have made significant progress in the field of humanoid robot whole-body control [1, 2, 3, 4, 5, 6]. Leveraging large-scale parallel simulations and domain randomization, policies are trained to absorb disturbances in mass, friction, and contact parameters, enabling zero-shot transfer to the real robot. However, RL controllers often neglect or oversimplify interactive forces. To meet the practical needs of humanoid robots in tasks like heavy-load manipulation and high-altitude operation, precise and robust motion control is essential in environments with strong external forces and dynamic changes.

When humanoid robots subject a strong collision or physical contact, RL controllers often exhibit instability. Specifically, current RL methods primarily use high-level commands such as moving velocity, root height, or predefined trajectories for control, which can overcome some random disturbances. However, when subjected to human intervention or significant contact with the environment, the lack of explicit modeling of contact dynamics often makes it difficult for the robot to maintain balance, potentially causing safety hazards [7, 8]. For example, in high-altitude operations, ropes are required for assistance, but their interference significantly affects the stability of the robot. In heavy-load scenarios, large payloads greatly reduce balanced behavior, placing severe demands on the load-bearing capacity of the hand.

To enhance the stability of control strategies under human intervention or significant external disturbances, this paper introduces HAFO, a force-adaptive control framework grounded in explicit dynamic modeling. HAFO employs a dual-agent strategy that decouples the control of the upper and lower bodies. The lower-body strategy focuses on robust locomotion to maintain gait stability under strong external disturbances. The upper-body strategy emphasizes precise control and real-time upper-body manipulation under external force disturbances. We utilize a spring-damping mechanical system to simulate interaction mechanics modeling. Meanwhile, we progressively increase external forces through a curriculum-learning schedule and randomize the point of force application, systematically enhancing the strategy's generalization to pulling forces, heavy load, and thrust disturbances. Our contributions are as follows:

- 1) A dual-agent reinforcement learning framework enabling the collaborative evolution of the upper and lower bodies under large external disturbances is proposed. The lower-body strategy is responsible for robust locomotion, and the upper-body strategy focuses on precise manipulation. Both strategies share the same state space. Through a coupling-adversarial mechanism, the system's stability is significantly improved, ultimately achieving whole-body collaborative control.
- 2) A Spring-Damping dynamic model has been developed, which explicitly models the external pulling force, as equivalent spring-damper forces acting on the robot body. During model training, a carefully designed progressive curriculum learning strategy is implemented, gradually increasing the spring-damper forces, enabling the policy gradually adapt to external disturbances. The RL policy autonomously evolves force-adaptive control modes for ground locomotion and aerial suspension, and spontaneously generates mode-switching behaviors based on environmental feedback, without relying on explicit state machines or predefined switching logic.
- 3) Experimental results demonstrate that the HAFO policy enables adaptive force control across multiple environments, exhibiting stable and precise motion capabilities under single or dual-hand loads. Moreover, HAFO is the first locomotion-control strategy to achieve stable operation and safe startup under rope-suspension conditions, representing preliminary exploratory work for humanoid robot applications in high-altitude scenarios.

2. Related Work

2.1. Whole-body control based on reinforcement learning

Object handling and assembly tasks demand whole-body coordination of a humanoid, which drastically increases control complexity. Traditional dynamics modeling has demonstrated good control performance in structured scenarios for legged robots [9, 10, 11, 12, 13, 14, 15, 16, 17]. However, the intrinsic under-actuation of humanoid robots and the variability of real-world environments make it challenging to accurately describe the dynamics of humanoid robots [1, 2, 3, 4, 6, 7, 8, 18, 19, 20, 21, 22, 23, 24, 25, 26, 27, 28, 29, 30, 31, 32]. Recently, some technical solutions based on reinforcement

learning provide new ideas for the whole-body control of humanoid robots. Common approaches include Lower-RL-Upper-IK and Monolithic-Whole-body-RL. These two paradigms solve the challenge of whole-body motion control of humanoid robots from different perspectives.

In terms of Lower-RL-Upper-IK paradigm, Ben et al. [18] proposed the Homie, which employs curriculum learning to dynamically adjust the motion tracking threshold, allowing the policy to progressively adapt to highdifficulty motions during training. Additionally, the Homie controller develops an isomorphic exoskeleton cockpit to achieve precise whole-body control of the robot. Liao et al. [27] designed a scalable and high-quality motion tracking framework called BeyondMimic, which can transform kinematic references into robust and highly dynamic robot motions. Through distillation, it integrates the trained motions into a single policy, enabling flexible combination of multiple skills during testing and achieving goal-driven control using only simple cost functions. By combining large-scale human motion data with reinforcement learning, Cheng et al. [19] encourage the robot's upper body to imitate the reference motion, while relaxing the imitation constraints on its two legs, enabling the robot to achieve expressive movements. The Mobile-TeleVision proposed by Lu et al. [23] introduces the predictive motion prior (PMP), which encodes multi-modal motion features through conditional variational autoencoder (CVAE) to guide the reinforcement learning strategy generates dynamic motions. For the Monolithic-Whole-body-RL paradigm, Xie et al. [28] proposed a KungfuBot, which introduces foot-ground contact states and a motion-phase signal to accurately imitate highly dynamic wushu movements. He et al. [2] proposed the OmniH2O teleoperation system, which integrates a teacher-student distillation framework to transfer knowledge from a privileged teacher policy to the deployed policy, enabling efficient and stable motion control of the robot in real-world environments. He et al. [21] proposed ASAP, which significantly enhances a robot's adaptability in complex environments by leveraging a pretrained motion tracking policy with a residual action model trained using real-world data.

Although the humanoid robot whole-body motion control has made remarkable progress in the above research, the existing methods still face many challenges. On the one hand, the Lower-RL-Upper-IK paradigm adopts the control mode of the upper-body open loop, which is difficult to perceive and adapt to the external interference in real time, on the other hand, the Monolithic-Whole-body-RL paradigm controls whole-body joints through a single controller, but due to the weak task goal correlation between upper-limb

manipulation and lower-limb walking, it is prone to overfitting.

2.2. Force-adaptive control

Humanoid robots inevitably experience continuous disturbances from external forces in real-world environments. However, existing research on force-adaptive control is relatively scarce. In the field of manipulation, hybrid position and force control methods are widely used. However, given the uncertainty of the interaction points between humanoid robots and the environment, the interaction forces are difficult to measure accurately using force sensors, which makes it challenging to directly apply these methods to legged robots.

Portela [33] et al. first introduced the force-adaptive control objective for quadruped robots, which significantly improved the force interaction capability of the end effector. However, the model requires explicit switching between position mode and force mode, and assumes the system is in a quasi-static state, making it difficult to handle dynamic and unknown disturbances. Forceadaptive control in humanoid robots presents several challenges. Specifically, there is significant dynamic coupling between the upper and lower limbs, joint torques are constrained by strict limitations, and the mass distribution is uneven. These characteristics make force-adaptive control particularly complex [34, 35, 36]. It is particularly noteworthy that FALCON designed a 3D force curriculum, which maximizes the force adaptability while ensuring the feasibility of joint torques [6]. Li et al. [37] introduced a force-adaptive torso-tilt reward, which maintains balance and effectively transmits force through torso tilting and center-of-gravity adjustment, generating greater pulling forces in high-intensity force interaction tasks. Kuo et al. [38] proposed a hybrid control method combining the Artificial Rabbit Optimization (ARO) algorithm with an MLP neural network. Through multi-angle impact experiments on flat and sloped terrain, they verified that the method can quickly adapt to external forces and effectively maintain balance. Existing model-based methods rely on precise modeling of pre-planned force trajectories, which restricts their generalization capability in unknown environments, rendering them inadequate for adapting to dynamically changing conditions [39]. In contrast, estimation-based approaches [40] are only applicable under quasi-static conditions and fail to effectively address force adaptive control in dynamic loco-manipulation tasks.

Although existing studies have explored force adaptive control for humanoid robots, most focus on relatively simple scenarios. Moreover, studies

implementing force adaptive control on humanoid robots are notably sparse. In this paper, we propose a force adaptation whole-body control (HAFO) strategy. Through explicit modeling of external disturbances, the proposed strategy endows humanoid robots with force-adaptive capability under challenging conditions such as heavy loads and pulling disturbances.

3. Method

Humanoid robot motion control requires coordinated movement of whole-body joints. Traditional whole-body control methods (WBC) use a single strategy to output the target joint angles for the entire body. However, the lack of strong coupling between upper and lower bodies tasks leads to inefficient sample utilization, making prone to overfitting. To maximize the exploration efficiency of reinforcement learning, this paper proposes the HAFO architecture shown in Fig. 1, in which a dual-agent reinforcement-learning framework drives the co-evolution of upper and lower bodies control strategies. Moreover, during the training process, a variety of dynamic disturbance factors are explicitly introduced to achieve stable force-adaptive control.

3.1. Dual-agent learning framework

We decompose the total DOFs of the humanoid into upper and lower bodies, $n_{\text{dof}} = \text{Upper}_{\text{dof}} + \text{Lower}_{\text{dof}}$, where Upper_{dof} is controlled by upper-body strategy π_{Upper} ($a_{\text{Upper}} \mid s$), Lower_{dof} is controlled by the lower-body strategy π_{lower} ($a_{\text{lower}} \mid s$). The dual-agent reinforcement learning strategy is trained using the Proximal Policy Optimization (PPO) algorithm [41] and shares the same state space $s_t = \left[s_t^{\text{prop}}, c^l, g^u\right]$, enabling both agents to consider the information of whole-body joints and achieve coordinated control. Among them, the $s_t^{\text{prop}} = \left[q_t, \dot{q}_t, \omega_t, gv_t, a_{t-1}\right]$ represents the body perception information of the robot, the $c^l = \left[\hat{v}_{x,t}, \hat{v}_{y,t}, \hat{\omega}_{yaw}, t\right]$ represents the command information for the lower-body strategy, and the $g^u \in \mathbb{R}^{14}$ represents the command information for the upper-body strategy.

The dual-agent policy is formulated as a dual-objective optimization problem. The value functions (V^l, V^u) corresponding to the upper and lower body policies (π^l, π^u) , and the rewards obtained can be represented as $(r^l(s, a^l, a^u), r^u(s, a^1, a^u))$. The two strategies optimize the policies by maximizing the cumulative rewards [42],

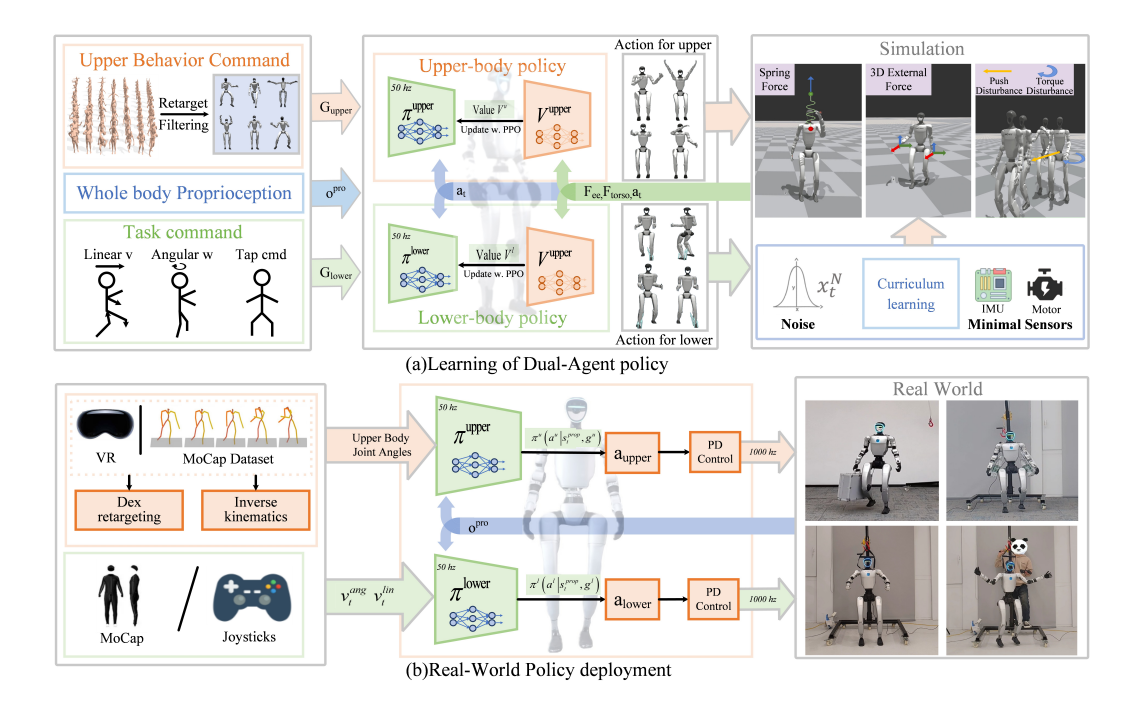


Figure 1: Overview of the HAFO model. (a) Policy training. A dual-agent strategy with decoupled upper and lower bodies is adopted, where the lower-body policy takes root linear and angular velocities as command inputs, and the upper-body policy uses reference joint trajectories as command inputs. Meanwhile, various explicit dynamic perturbations are introduced at key locations to enhance the system's robustness and adaptability. (b) Strategy deployment. A humanoid robot control system based on teleoperation is developed, employing an efficient inverse kinematics algorithm to compute the robot's joint angles in real time with high precision, enabling efficient loco-manipulation tasks.

$$\begin{cases}
\max_{\theta_u} \mathbb{E}_{\pi_{\text{upper}}} \left[\sum_{t=0}^{T-1} \gamma^t r_t \right] & \text{(upper policy)} \\
\max_{\theta_l} \mathbb{E}_{\pi_{\text{lower}}} \left[\sum_{t=0}^{T-1} \gamma^t r_t \right] & \text{(lower policy)}
\end{cases}$$
(1)

3.2. Robust lower-body movement under external forces

Robust locomotion of humanoid robots is still a formidable challenge, primarily due to the complexity of the floating base and the instability caused by high inertia. This difficulty is compounded when payloads are placed on the upper body, which both increases the overall inertia and introduces additional modeling uncertainty, further complicating control design.

For the lower limb strategy $\pi^l: C^l \times S \mapsto A^l$, we employ a variety of external disturbances during the training process to enhance the robot's robustness, including adversarial upper-body perturbations and high-frequency random pushing disturbances.

3.3. Upper-body motion generation based on imitation learning

The demonstration data for the upper-body policy come from the AMASS human-motion dataset after feasibility filtering. Following PHC [24], we retarget human poses to humanoid poses and apply filtering to suppress jitter and discontinuities. Instead of open-loop replay, we train a reinforcement-learning policy for the upper-body that can adapt to changing environments, improve whole-body coordination. The upper-body policy $\pi^{\rm u}:C^{\rm u}\times S\mapsto A^{\rm u}$ is trained in conjunction with the lower-body policy $\pi^{\rm l}:C^{\rm l}\times S\mapsto A^{\rm l}$, and the state space of the upper-body strategy contains the state of the whole body. To improve the load capacity of the humanoid robot, we apply disturbances to the robot's end-effectors in the form of random 3D spatial forces [6].

When the training of the upper-body strategy, samples are randomly taken from the offline dataset $M_t = \mathbf{q}_{1:T}^{\text{upper}}$ to keep the data variety and prevent overfitting to local patterns. To reduce the learning difficulty of the lower-body policy, we design a progressive imitation curriculum that guides the network gradually learns the upper-body reference trajectory, progressing from simple to complex and coarse to fine.

$$q_{\text{curr}}^{u}(t) = q_0(t) + \alpha_i \left(q_{\text{tar}}^{u}(t) - q_0(t) \right)$$
 (2)

Among them, $q_0(t)$ represents the actual joint angle vector at time t, $q_{tar}(t)$ is the target joint angle vector of the upper-body at that time t, and $\alpha_i \in [0, 1]$ is the course gain coefficient, which is used to modulate the motion amplitude of the upper-body reference trajectory.

We adopt an asymmetric actor-critic training approach, where the critic network used both observable information o_t and privileged information $o_o^{\text{priv}} = \{F_{\text{ee}}, F_{\text{torso}}, v_{\text{lin}}\}$ to achieve accurate value estimation, while the actor network relies solely on the observable information of the physical machine.

3.4. Impedance control

In complex and unpredictable environments, a precise and stable control system is essential for achieving task objectives. To enhance the robustness of humanoid robots under unknown external disturbances, this paper proposes a pulling-force modeling mechanism based on impedance control [43, 44, 45], explicitly incorporating the pulling force interaction process into the training loop. We extend the principle of impedance control to humanoid robots, aiming to regulate the robot's body dynamics through a virtual spring-damper model, the corresponding dynamic model is given by

$$m\ddot{\mathbf{x}} = K_{\mathrm{p}} \left(\mathbf{x}_{\mathrm{des}} - \mathbf{x} \right) + K_{\mathrm{d}} \left(\dot{\mathbf{x}}_{\mathrm{des}} - \dot{\mathbf{x}} \right) + \mathbf{f}_{\mathrm{ext}}$$
 (3)

Where K_p and K_d represent the stiffness and damping of the virtual spring-damper system, $(\mathbf{x}_{\text{des}}, \dot{\mathbf{x}}_{\text{des}})$ denotes the desired position and velocity.

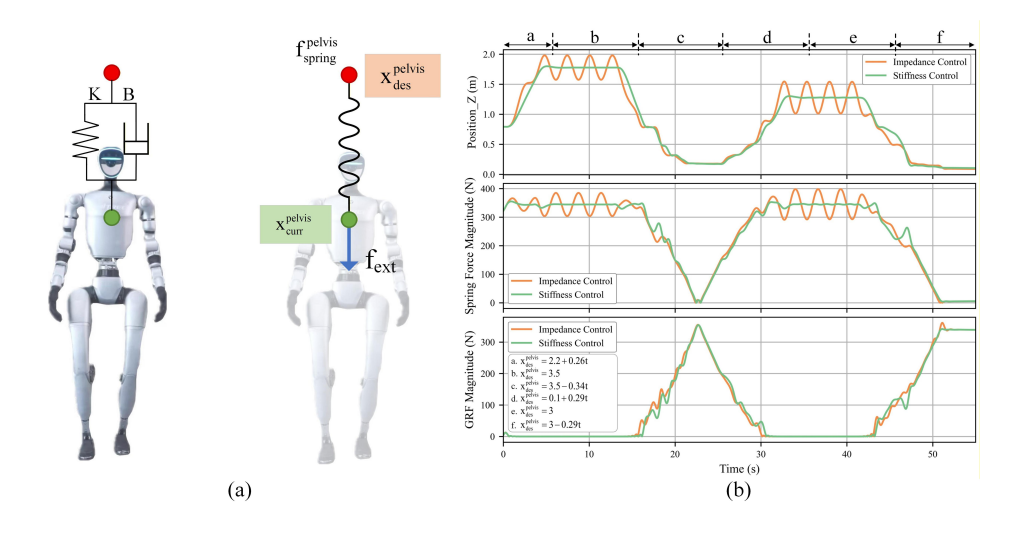


Figure 2: Impedance-control model and performance analysis. (a) Spring-damper model schematic on the humanoid robot. (b)Pelvis position, spring force, and ground-reaction force versus $\mathbf{X}_{\mathrm{des}}^{\mathrm{pelvis}}$ displacement for Impedance and stiffness controllers.

Leveraging a spring-damper model, we accurately capture the mechanics of external tensile force. By progressively adjusting the $\mathbf{X}_{\text{des}}^{\text{pelvis}}$, the tensile force is tuned to achieve stable position control. Comparative tests show that stiffness control produces pronounced oscillations relative to impedance control, confirming the critical role of the damping term in enhancing stability and precision. During training, we randomize the force application position, cycle, and dropout timing, significantly enhancing policy generalization.

4. Simulation Experiments

In this section, we conduct a series of force-interaction simulation experiments and comprehensively evaluated the effectiveness of the proposed HAFO framework through quantitative comparisons with the baseline methods. All simulations are conducted in MuJoCo via zero-shot transfer from Isaac Gym. The cross-platform validation approach effectively mitigates overfitting risks inherent to a single simulator, thereby effectively verifying policy robustness.

4.1. Force adaptive control under hand-induced disturbances

To evaluate the stability performance of the model under external disturbances, we apply forces of different directions and magnitudes to the robot's end-effectors in the simulation environment, with the force magnitude incrementally increasing from 10N to 50N. During the force disturbance process, the robot executed random velocity commands (linear velocity range [-0.5, 0.5] m/s, angular velocity range [-0.5, 0.5] rad/s) and performed diverse upper-limb motion sequences sampled from a subset of the AMASS dataset. We test key indicators such as the upper-body motion tracking error and velocity tracking error. Motion tracking error is measured by calculating the difference between the actual joint angles and the target joint angles, and velocity tracking error is measured by calculating the difference between the actual velocity and the target velocity.

Upper-body motion tracking error:

$$E_{\text{error}}^{\text{upper}} = \frac{1}{T} \sum_{t=1}^{T} \left| q_t^{\text{upper}^*} - q_t^{\text{upper}} \right| \tag{4}$$

Velocity tracking error:

$$E_{\text{error}}^{\text{vel}} = \frac{1}{T} \sum_{t=1}^{T} \left| v_t^{\text{lin,ang}^*} - v_t^{\text{lin,ang}} \right| \tag{5}$$

The velocity tracking error E_{error}^{vel} (m/s) and upper-body motion tracking error E_{error}^{upper} (rad) are computed as the average values over a complete iteration. To verify the effectiveness of the proposed Force-Adaptive Control strategy, we select two representative benchmarks:

(i) Upper-OL-Lower-RL: a decoupled policy with open-loop upper-body control and RL-driven lower-body control [18].

Table 1: Policy Tracking Performance Evaluation. We assessed the upper-body motion tracking performance and lower-body velocity tracking performance of different policies under three external force magnitudes applied to each hand (N-Force: 10 N, S-Force: 30 N, M-Force: 50 N). These metrics reflect the force adaptability of the policies under external disturbance, where "/" indicates task failure.

Methods	$ m E_{tracking}^{upper} \downarrow$			$ m E_{tracking}^{root} \downarrow$		
Welliods	S-Force	N-Force	L-Force	S-Force	N-Force	L-Force
Upper-OL-Lower-RL	$0.36 {\pm} 0.03$	$0.74 {\pm} 0.04$	$1.23{\pm}0.07$	$0.32 {\pm} 0.04$	$0.53 {\pm} 0.10$	1.52 ± 0.22
${\it Upper-FIX-Lower-RL}$	$0.55 {\pm} 0.06$	/	/	$0.52{\pm}0.09$	/	/
HAFO w.o. DA	$0.34 {\pm} 0.08$	$0.66 {\pm} 0.11$	$1.32 {\pm} 0.17$	$0.50 {\pm} 0.02$	$0.55{\pm}0.03$	$0.77 {\pm} 0.07$
HAFO w.o. Force	$0.42 {\pm} 0.03$	$0.60 {\pm} 0.03$	$1.36 {\pm} 0.11$	$0.36 {\pm} 0.03$	$0.54{\pm}0.08$	$0.92 {\pm} 0.06$
HAFO	$0.22{\pm}0.04$	$0.41 {\pm} 0.03$	$0.46{\pm}0.04$	$0.33 {\pm} 0.02$	$0.48 {\pm} 0.03$	$0.53 {\pm} 0.05$

(ii) Upper-FIX-Lower-RL: a lower-body motion strategy with the upper body fixed [46].

Furthermore, we conduct ablation experiments to quantify the contribution of each HAFO module. We sequentially ablate (i) the dual-agent architecture, retaining only the lower-body agent (w.o. DA), and (ii) the force-adaptation module (w.o. Force). As shown in Table 1, comparative experiments demonstrate that HAFO achieves the most accurate tracking performance in terms of velocity tracking and upper-body angle following. Upper-FIX-Lower-RL simplifies training by fixing the upper-body and relying exclusively on lower-body control for locomotion; however, it cannot guarantee system stability when the upper-body execute dynamic motions. Notably, the policy demonstrates a more pronounced performance advantage as the hand-applied external force increases. Furthermore, ablation results demonstrate that removing either module leads to performance degradation. The random upper-body motion introduced during training serves as an adversarial perturbation source, potentially compelling the lower-body policy to learn more generalized dynamic compensation mechanisms. Meanwhile, force curriculum learning effectively enhances the dual-agent's robustness and adaptability under perturbations.

4.2. Force adaptive control under rope suspension

We conduct a comprehensive evaluation of the strategy's force adaptability under suspension, focusing on upper-body motion tracking error, action smoothness. Upper-body motion tracking error $E_{\rm tracking}^{\rm upper} \downarrow ({\rm rad})$ is evaluated by the deviation between target joint angles and actual joint angles,

Table 2: The comparison of different methods in terms of action smoothness and upper-body motion tracking error.

Methods	$\Delta a \downarrow$	$\mathrm{E}_{\mathrm{tracking}}^{\mathrm{upper}} \downarrow$	
Upper-OL-Lower-RL	$2.49{\pm}2.38$	$0.27{\pm}0.11$	
Upper-FIX-Lower-RL	5.66 ± 4.50	$0.29 {\pm} 0.15$	
HAFO w.o. DA	1.60 ± 0.49	$0.27{\pm}0.24$	
${ m HAFO}$ -w/o- force	$4.52{\pm}1.77$	1.16 ± 0.66	
HAFO(Ours)	$0.38 {\pm} 0.16$	$0.20{\pm}0.04$	

while action smoothness $\Delta a \downarrow (m/s)$ is represented by motion smoothness. Under dynamic disturbances during suspension, significant variations occur in the robot's motion states, including angular velocity, linear velocity, body posture, and foot-ground contact. The HAFO policy effectively addresses uncertainties in suspension dynamics through real-time environmental feedback and adaptive behavior adjustment, demonstrating consistent reliability across various lifting and landing scenarios. As shown in Table 2, using the HAFO policy, Upper-body motion tracking error is 0.38, action smoothness is 0.20, significantly enhancing force adaptability in rope suspension scenarios and outperforming existing strategies. Notably, the HAFO strategy shows significant compliance and stability during lifting and landing transitions, which fully validates that the dual-agent collaborative mechanism combined with force curriculum learning enables systematic and precise identification of suspension dynamics characteristics. This significantly enhances force adaptability and robustness in rope suspension scenarios. Furthermore, ablation studies demonstrate that, despite undergoing force curriculum learning, HAFO w.o. DA employs open-loop control for the upper limbs, lacking active adaptability and resulting in significant performance degradation.

4.3. Force-Adaptive Control under Thrust Disturbance

To systematically evaluate policy robustness against thrust perturbations, we designed two disturbance rejection experiments: applying sustained constant forces and one-second transient forces along eight directions in the horizontal plane, progressively increasing force magnitude until loss of stability. As shown in Fig 3, HAFO achieved greater tolerance to external disturbances in most directions compared to HAFO w.o. DA, HAFO w.o. Force, and

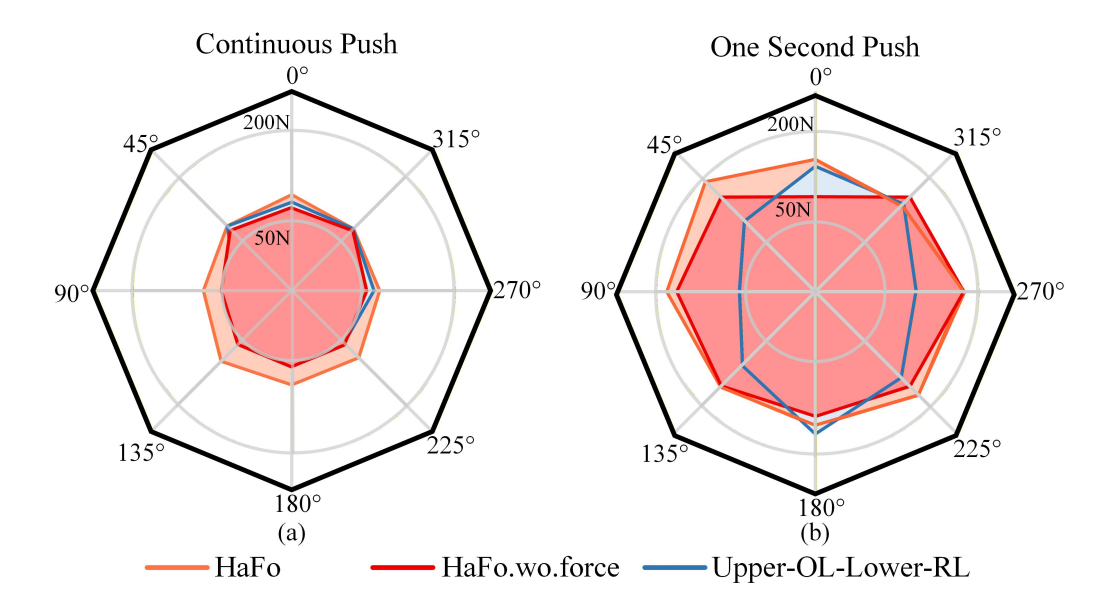


Figure 3: Policy performance under varied external disturbances. (a) Performance under continuous constant-force disturbances applied from multiple directions. (b) Performance under one-second transient force disturbances from multiple directions.

the baseline strategy, indicating that adversarial upper-body training and the force curriculum both enhance the robot's force adaptation under thrust perturbations.

5. Real-world experiments

We deployed the HAFO strategy on physical Unitree G1 humanoid robot and conducted a series of hardware experiments. As shown in Fig.4, the HAFO controller accomplished multiple force interaction tasks, collectively validating our method's technical performance and practical applicability on the physical robot.

5.1. Loco-manipulation under hand loads

To evaluate the robot's motion performance under load, we conduct experiments with both single-hand and dual-hand loads. In the experiment, we record the velocity tracking error and upper-body motion tracking error respectively. As shown in Table 3, whether the robot carried the load with one hand or both, HAFO maintain the lowest velocity-tracking and upper-limb joint errors, outperforming the baseline methods.

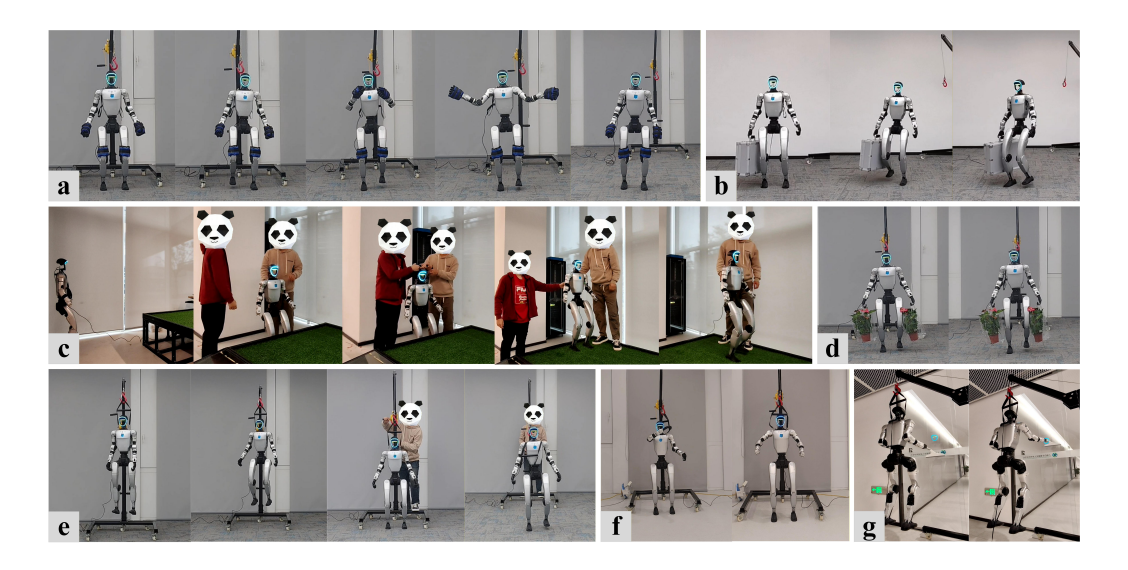


Figure 4: HAFO enables force-adaptive control for humanoid robots across multiple scenarios. (a) Whole-body locomotion with sandbag loads. (b) Walking while carrying a box with one hand. (c) Being lifted onto an elevated platform and resuming locomotion. (d) Walking while carrying flower pots with both hands. (e) Policy deployment in a suspended state. (f) Performing dance movements. (g) Window cleaning while suspended by ropes.

5.2. Stable control under suspension

Traditional policy initialization schemes typically require robots to sequentially execute the series of procedures: foot-ground contact, posture adjustment, policy execution, and rope release. This process is relatively cumbersome, and sustained external disturbances from the rope readily leads to robot instability. This experiment validates the feasibility of suspended startup. As shown in Table 4, the HAFO controller can initiate directly from a rope-suspended state and rapidly reach steady state, significantly simplifying the policy deployment process. Under the dynamic interference of rope tension, significant changes occurred in the robot's locomotion states, including linear velocity, angular velocity, body posture, and foot-ground contact, which lead to leads to instability in the Baseline policy. In contrast, the HAFO policy leverages environmental feedback for adaptive compensation, robustly maintaining locomotion stability.

To verify the force adaptability in the rope suspension scenario, we simulate the typical suspended operation conditions, and systematically test the whole process of lifting, operating and landing. In the lifting phase, the robot is lifted from the ground, and its posture stability is monitored in real time.

Table 3: Policy Tracking Performance Evaluation in Real-world robot. We evaluate upperbody motion tracking error and lower-body velocity tracking error of different policies across difficulty hand-loading modes (1-kg load in one hand, 1-kg load in each hand).

Methods	One han	d loads	Two hand loads		
Methods	$E_{tracking}^{upper} \downarrow$	$E_{ m tracking}^{ m root}$	$E_{tracking}^{upper} \downarrow$	$E_{\text{tracking}}^{\text{root}}$	
Upper-OL-Lower-RL	$0.28 {\pm} 0.05$	0.49 ± 0.03	0.53 ± 0.08	0.50 ± 0.04	
HAFO w.o. DA	$0.45{\pm}0.08$	$0.58 {\pm} 0.05$	$0.64 {\pm} 0.12$	$0.57{\pm}0.05$	
HAFO w.o. Force	$0.40 {\pm} 0.06$	$0.43 {\pm} 0.08$	$0.54 {\pm} 0.07$	$0.44 {\pm} 0.11$	
HAFO	$0.16{\pm}0.05$	$0.40 {\pm} 0.04$	$0.39 {\pm} 0.03$	$0.41 {\pm} 0.03$	

Table 4: Policy performance evaluation across different task scenarios. We assessed motion smoothness and upper-limb tracking error for each task scenario.

Methods	$\Delta a \downarrow$	$\mathrm{E}_{\mathrm{tracking}}^{\mathrm{upper}} \downarrow$	
Hang on start	0.19 ± 0.01	0.13 ± 0.01	
high-altitude work	$0.43 {\pm} 0.05$	$0.21 {\pm} 0.03$	

After entering the operation phase, the robot performs the teleoperation tasks in the suspended state. Finally, the robot achieves a stable bipedal stance following touchdown. We compare with the existing scheme, and finally only the HAFO completed the final experiment, the results are shown in Table 4. We show the application potential of HAFO in high-rise outdoor dangerous scenes, and provide new ideas and methods for the practical application of robots in the future.

6. Conclusion

In this paper, we propose HAFO, a force-adaptive control framework for humanoid robots. HAFO employs a dual-agent control strategy and explicitly introduces various dynamic disturbances, achieving stable motion control and precise motion imitation. During the model training, a spring-damper system is established, and fine-grained tension control of the pulling force is achieved through manipulation of virtual springs. At the same time, HAFO employs asymmetric Actor-Critic architecture wherein the critic-

network is granted full access to privileged state variables, thereby furnishing a more accurate approximation of state-action value. Experimental results demonstrate that the proposed strategy enables the humanoid robot to exhibit strong adaptability under challenging conditions such as heavy loading, thrust disturbance and rope suspension, providing robust support for solving substantial force interaction tasks in real-world applications.

7. Acknowledgments

This work was supported in part by the National Natural Science Foundation of China under Grant 62088101, Grant 62403366, Grant 62473294, and Grant 62403363; in part by Shanghai Municipal Science and Technology Major Project under Grant 2021SHZDZX0100.

References

- [1] J. He, C. Zhang, F. Jenelten, R. Grandia, M. Bächer, M. Hutter, Attention-based map encoding for learning generalized legged locomotion, Science Robotics 10 (2025) eadv3604.
- [2] T. He, Z. Luo, X. He, W. Xiao, C. Zhang, W. Zhang, K. M. Kitani, C. Liu, G. Shi, Omnih2o: Universal and dexterous human-to-humanoid whole-body teleoperation and learning, in: 2nd Workshop on Dexterous Manipulation: Design, Perception and Control (RSS), 2024.
- [3] I. Radosavovic, T. Xiao, B. Zhang, T. Darrell, J. Malik, K. Sreenath, Real-world humanoid locomotion with reinforcement learning, Science Robotics 9 (2024) eadi9579.
- [4] L. Yang, X. Huang, Z. Wu, A. Kanazawa, P. Abbeel, C. Sferrazza, C. K. Liu, R. Duan, G. Shi, Omniretarget: Interaction-preserving data generation for humanoid whole-body loco-manipulation and scene interaction, arXiv preprint arXiv:2509.26633 (2025).
- [5] C. Fu, K. Chen, Gait synthesis and sensory control of stair climbing for a humanoid robot, IEEE Transactions on Industrial Electronics 55 (2008) 2111–2120.

- [6] Y. Zhang, Y. Yuan, P. Gurunath, T. He, S. Omidshafiei, A.-a. Aghamohammadi, M. Vazquez-Chanlatte, L. Pedersen, G. Shi, Falcon: Learning force-adaptive humanoid loco-manipulation, arXiv preprint arXiv:2505.06776 (2025).
- [7] M. Sombolestan, Q. Nguyen, Adaptive-force-based control of dynamic legged locomotion over uneven terrain, IEEE Transactions on Robotics 40 (2024) 2462–2477.
- [8] B. Xu, H. Weng, Q. Lu, Y. Gao, H. Xu, Facet: Force-adaptive control via impedance reference tracking for legged robots, arXiv preprint arXiv:2505.06883 (2025).
- [9] J. Carpentier, N. Mansard, Multicontact locomotion of legged robots, IEEE Transactions on Robotics 34 (2018) 1441–1460.
- [10] D. Song, P. Fernbach, T. Flayols, A. Del Prete, N. Mansard, S. Tonneau, Y. J. Kim, Solving footstep planning as a feasibility problem using l1-norm minimization, IEEE Robotics and Automation Letters 6 (2021) 5961–5968.
- [11] J. Wang, S. Kim, S. Vijayakumar, S. Tonneau, Multi-fidelity receding horizon planning for multi-contact locomotion, in: 2020 IEEE-RAS 20th International Conference on Humanoid Robots (Humanoids), IEEE, 2021, pp. 53–60.
- [12] P. Fernbach, S. Tonneau, O. Stasse, J. Carpentier, M. Taïx, C-croc: Continuous and convex resolution of centroidal dynamic trajectories for legged robots in multicontact scenarios, IEEE Transactions on Robotics 36 (2020) 676–691.
- [13] M. Jin, J. Lee, N. G. Tsagarakis, Model-free robust adaptive control of humanoid robots with flexible joints, IEEE Transactions on Industrial Electronics 64 (2016) 1706–1715.
- [14] J. Ding, C. Della Santina, T. L. Lam, J. Pang, X. Xiao, N. G. Tsagarakis, Y. Huang, Robust humanoid locomotion via sequential stepping and angular momentum optimization, IEEE Transactions on Industrial Electronics (2024).

- [15] H. Yin, H. Jin, F. Ju, J. Liu, M. Zhao, J. Zhao, Kinematic control of humanoid upper body robot using virtual flexible joint dynamics primitive and quasi-sliding mode observer, IEEE Transactions on Industrial Electronics (2025).
- [16] M. Farhat, Y. Kali, M. Saad, M. H. Rahman, R. E. Lopez-Herrejon, New fixed-time observer-based model-free fixed-time sliding mode of joint angle commanded nao humanoid robot, IEEE Transactions on Control Systems Technology (2024).
- [17] Q. Wang, Q. Li, M. Zhao, Fast terrain-adaptive motion of humanoid robots based on model reference one-step-ahead predictive control, IEEE Transactions on Control Systems Technology 31 (2023) 2819–2834.
- [18] Q. Ben, F. Jia, J. Zeng, J. Dong, D. Lin, J. Pang, Homie: Humanoid loco-manipulation with isomorphic exoskeleton cockpit, in: RSS 2025 Workshop on Whole-body Control and Bimanual Manipulation: Applications in Humanoids and Beyond, 2025.
- [19] X. Cheng, Y. Ji, J. Chen, R. Yang, G. Yang, X. Wang, Expressive whole-body control for humanoid robots, arXiv preprint arXiv:2402.16796 (2024).
- [20] Z. Fu, Q. Zhao, Q. Wu, G. Wetzstein, C. Finn, Humanplus: Humanoid shadowing and imitation from humans, arXiv preprint arXiv:2406.10454 (2024).
- [21] T. He, J. Gao, W. Xiao, Y. Zhang, Z. Wang, J. Wang, Z. Luo, G. He, N. Sobanbab, C. Pan, et al., Asap: Aligning simulation and real-world physics for learning agile humanoid whole-body skills, arXiv preprint arXiv:2502.01143 (2025).
- [22] Y. Li, Y. Lin, J. Cui, T. Liu, W. Liang, Y. Zhu, S. Huang, Clone: Closed-loop whole-body humanoid teleoperation for long-horizon tasks, arXiv preprint arXiv:2506.08931 (2025).
- [23] C. Lu, X. Cheng, J. Li, S. Yang, M. Ji, C. Yuan, G. Yang, S. Yi, X. Wang, Mobile-television: Predictive motion priors for humanoid whole-body control, in: 2025 IEEE International Conference on Robotics and Automation (ICRA), IEEE, 2025, pp. 5364–5371.

- [24] Z. Luo, J. Cao, K. Kitani, W. Xu, et al., Perpetual humanoid control for real-time simulated avatars, in: Proceedings of the IEEE/CVF International Conference on Computer Vision, 2023, pp. 10895–10904.
- [25] J. Shi, X. Liu, D. Wang, O. Lu, S. Schwertfeger, F. Sun, C. Bai, X. Li, Adversarial locomotion and motion imitation for humanoid policy learning, arXiv preprint arXiv:2504.14305 (2025).
- [26] C. Tessler, Y. Guo, O. Nabati, G. Chechik, X. B. Peng, Maskedmimic: Unified physics-based character control through masked motion inpainting, ACM Transactions on Graphics (TOG) 43 (2024) 1–21.
- [27] Q. Liao, T. E. Truong, X. Huang, G. Tevet, K. Sreenath, C. K. Liu, Beyondmimic: From motion tracking to versatile humanoid control via guided diffusion, arXiv preprint arXiv:2508.08241 (2025).
- [28] W. Xie, J. Han, J. Zheng, H. Li, X. Liu, J. Shi, W. Zhang, C. Bai, X. Li, Kungfubot: Physics-based humanoid whole-body control for learning highly-dynamic skills, arXiv preprint arXiv:2506.12851 (2025).
- [29] Y. Ze, Z. Chen, J. P. AraÚjo, Z.-a. Cao, X. B. Peng, J. Wu, C. K. Liu, Twist: Teleoperated whole-body imitation system, arXiv preprint arXiv:2505.02833 (2025).
- [30] T. Zhang, B. Zheng, R. Nai, Y. Hu, Y.-J. Wang, G. Chen, F. Lin, J. Li, C. Hong, K. Sreenath, et al., Hub: Learning extreme humanoid balance, arXiv preprint arXiv:2505.07294 (2025).
- [31] Y. Zhang, T. Liang, Z. Chen, Y. Ze, H. Xu, Catch it! learning to catch in flight with mobile dexterous hands, in: 2025 IEEE International Conference on Robotics and Automation (ICRA), IEEE, 2025, pp. 14385– 14391.
- [32] P.-H. Kuo, W.-C. Yang, P.-W. Hsu, K.-L. Chen, Intelligent proximal-policy-optimization-based decision-making system for humanoid robots, Advanced Engineering Informatics 56 (2023) 102009.
- [33] T. Portela, G. B. Margolis, Y. Ji, P. Agrawal, Learning force control for legged manipulation, in: 2024 IEEE International Conference on Robotics and Automation (ICRA), IEEE, 2024, pp. 15366–15372.

- [34] R. Martín-Martín, M. A. Lee, R. Gardner, S. Savarese, J. Bohg, A. Garg, Variable impedance control in end-effector space: An action space for reinforcement learning in contact-rich tasks, in: 2019 IEEE/RSJ international conference on intelligent robots and systems (IROS), IEEE, 2019, pp. 1010–1017.
- [35] C. C. Beltran-Hernandez, D. Petit, I. G. Ramirez-Alpizar, T. Nishi, S. Kikuchi, T. Matsubara, K. Harada, Learning force control for contact-rich manipulation tasks with rigid position-controlled robots, IEEE Robotics and Automation Letters 5 (2020) 5709–5716.
- [36] C. Chen, Z. Yu, H. Choi, M. Cutkosky, J. Bohg, Dexforce: Extracting force-informed actions from kinesthetic demonstrations for dexterous manipulation, IEEE Robotics and Automation Letters (2025).
- [37] G. Li, Q. Shi, Y. Hu, J. Hu, Z. Wang, X. Wang, S. Luo, Thor: Towards human-level whole-body reactions for intense contact-rich environments, arXiv preprint arXiv:2510.26280 (2025).
- [38] P.-H. Kuo, W.-C. Yang, Y.-S. Lin, C.-C. Peng, Artificial rabbits optimization-based motion balance system for the impact recovery of a bipedal robot, Advanced Engineering Informatics 63 (2025) 102965.
- [39] J. Li, Q. Nguyen, Kinodynamics-based pose optimization for humanoid loco-manipulation, arXiv preprint arXiv:2303.04985 (2023).
- [40] T. Mattioli, M. Vendittelli, Interaction force reconstruction for humanoid robots, IEEE Robotics and Automation Letters 2 (2016) 282–289.
- [41] J. Schulman, F. Wolski, P. Dhariwal, A. Radford, O. Klimov, Proximal policy optimization algorithms, arXiv preprint arXiv:1707.06347 (2017).
- [42] F. A. Oliehoek, C. Amato, et al., A concise introduction to decentralized POMDPs, volume 1, Springer, 2016.
- [43] N. Hogan, Impedance control: An approach to manipulation, in: 1984 American control conference, IEEE, 1984, pp. 304–313.
- [44] Y. Hou, Z. Liu, C. Chi, E. Cousineau, N. Kuppuswamy, S. Feng, B. Burchfiel, S. Song, Adaptive compliance policy: Learning approximate compliance for diffusion guided control, in: 2025 IEEE International Conference on Robotics and Automation (ICRA), IEEE, 2025, pp. 4829–4836.

- [45] J. Shi, C. Bai, H. He, L. Han, D. Wang, B. Zhao, M. Zhao, X. Li, X. Li, Robust quadrupedal locomotion via risk-averse policy learning, in: 2024 IEEE International Conference on Robotics and Automation (ICRA), IEEE, 2024, pp. 11459–11466.
- [46] Z. Zhang, C. Chen, H. Xue, J. Wang, S. Liang, Y. Liu, Z. Zhang, H. Wang, L. Yi, Unleashing humanoid reaching potential via real-world-ready skill space, arXiv preprint arXiv:2505.10918 (2025).